

Comprehensive Method for Angular Super-Resolution of Group Targets

B. A. Lagovsky^{*,a} and E. Y. Rubinovich^{**,b}

^{*}Russian Technological University, Moscow, Russia

^{**}Trapeznikov Institute of Control Sciences, Russian Academy of Sciences, Moscow, Russia

e-mail: ^arobertlag@yandex.ru, ^brubinvch@gmail.com

Received November 19, 2024

Revised April 5, 2025

Accepted April 7, 2025

Abstract—A comprehensive method is proposed to enhance the resolution and accuracy of radar angular measurements for detecting and determining the coordinates of objects in the form of closely spaced multiple aerial targets that cannot be resolved by direct observation. Solving this problem improves the quality of controlling various types of unmanned aerial vehicles (UAVs) located near such targets. The practical implementation of the method is particularly important in calculating and modeling flight trajectories of autonomous and controlled aerial vehicles when visual observation is difficult or ineffective. Mathematically, the problem reduces to solving Fredholm integral equations of the first kind of convolution type with additional constraints. Solutions with angular super-resolution are sought in the form of an expansion of the unknown function over chosen systems of orthogonal functions. For group targets with high object density, it is not always possible to obtain an adequate solution to this inverse problem. In such cases, enhancing the achievable super-resolution degree is proposed based on a new method called the separation method. It is based on excluding from the analyzed signal its component formed by reflection from one or several targets distinguished by some means. The use of nonlinear regression methods in research is justified. Results of numerical experiments on a mathematical model are presented and analyzed.

Keywords: Rayleigh criterion, angular super-resolution, stability of inverse problem solutions

DOI: 10.7868/S1608303225120033

1. INTRODUCTION

Angular super-resolution of a measurement or observation system refers to angular resolution capability exceeding the Rayleigh criterion. The Rayleigh criterion is the minimum angular distance θ_R between two point objects at which the measurement system can still register them separately:

$$\theta_R = \lambda/L, \quad (1)$$

where L is the linear size of the receiving system, λ is the wavelength used. The angle θ_R equals the antenna beamwidth $\theta_{0.5}$, defined at the level of received power reduction by a factor of 2.

In measurements of angular coordinates, the obtained resolution does not exceed the Rayleigh criterion. Results of digital signal processing using special algorithms allow systems to detail images of studied objects with accuracy down to a previously unknown angle $\theta_s < \theta_R$. The value θ_s depends on the signal-to-noise ratio (SNR) in the data, the digital processing method used, as well as the angular reflection (or radiation) characteristics of the signals from the studied objects. Achieved angular super-resolution improves measurement accuracy, enhances detection and identification

probability characteristics. It becomes possible to observe and measure coordinates of individual closely located objects within targets, called group targets, which previously, according to (1), merged into a single extended object.

Consequently, the obtained dynamic picture enables improving the effectiveness of controlling unmanned aerial vehicles (UAVs) operating in zones containing many other UAVs and UAV “swarms.”

Several dozen numerical methods for achieving super-resolution and their variations are known [1–7]. However, there is no single universal method for solving the super-resolution achievement problem. All methods and algorithms have various limitations. For example, for most methods, super-resolution can only be achieved at SNR above 20–25 dB. The most well-known methods [5–7] are effective only for solving one-dimensional problems. For two-dimensional problems, algorithms become significantly more complex [8] and do not allow real-time use.

For each specific problem, one should choose its own, most effective method for processing measurement or observation data under the given conditions. The quality of the obtained approximate solution can be improved by combining several new methods into a single comprehensive method. It is based on the sequential application, depending on the results obtained, of new specialized processing methods described in Sections 4–6.

2. PROBLEM FORMULATION

Let a large number of closely located UAVs be present in the surveillance zone of a radar station (ground-based or mounted on an aerial vehicle). A significant portion of objects, due to relatively small distances between them, are not angularly resolved by direct observation. In this case, they form a single large spatial object, i.e., a group target.

It is necessary to isolate the maximum possible number of individual objects in the surveillance zone and determine their coordinates. The characteristics of the measurement system and the received signal are assumed known.

Mathematical problem formulation.

Given: antenna pattern (AP) $F(\alpha, \varphi)$, the received signal $U(\alpha, \varphi)$ during scanning of the two-dimensional surveillance sector Ψ in the form of a linear integral transform:

$$U(\alpha, \varphi) = \int_{\Omega} F(\alpha - \alpha', \varphi - \varphi') I(\alpha', \varphi') d\alpha' d\varphi', \quad (2)$$

where Ω is an unknown two-dimensional angle within which signal sources are located, and $\Omega < \Psi$. It is required to find the angular distribution of the reflected signal amplitude $I(\alpha, \varphi)$, equal to zero outside the region Ω .

The problem of finding the function $I(\alpha, \varphi)$ represents an inverse problem, ill-posed in the sense of Hadamard, in the form of a Fredholm integral equation (IE) of the first kind. In such problems, the third condition of well-posedness—stability of solutions with respect to input data—is violated.

It is well known that the stability of inverse problems can be improved by using any additional data about the solution. Algebraic methods [9–15] are convenient for introducing various additional constraints into solutions. Furthermore, the mentioned methods are relatively noise-resistant, and their high speed allows real-time use. For the considered class of problems, they are the most promising.

3. REGULARIZATION OF THE PROBLEM USING THE ALGEBRAIC METHOD

Algebraic methods involve representing one- or two-dimensional solutions (2) as expansions over a given orthogonal system of functions in the region of source location.

Consider a one-dimensional problem when scanning is performed along one coordinate. Generalization of the obtained results to the two-dimensional case presents no fundamental difficulties.

Following the ideology of algebraic methods, the desired solution $I(\alpha)$ can be represented as

$$I(\alpha) = \sum_{m=1}^{\infty} b_m g_m(\alpha) \cong \sum_{m=1}^M b_m g_m(\alpha), \quad (3)$$

where $g_m(\alpha)$, $m = 1, \dots, M$ is a chosen finite system of functions orthogonal in the region Ω , b_m are the desired expansion coefficients of $I(\alpha)$ in a series. Then the received signal (2) can be represented as

$$U(\alpha) = \sum_{m=1}^{\infty} b_m G_m(\alpha) \cong \sum_{m=1}^M b_m G_m(\alpha), \quad G_m(\alpha) = \int_{\Omega} F(\alpha - \alpha') g_m(\alpha') d\alpha', \quad (4)$$

and it turns out to be a superposition of non-orthogonal functions $G_m(\alpha)$. Thus, the inverse problem becomes parameterized. Its approximate solution reduces to finding the vector of coefficients B with elements b_m , which are determined from a system of linear algebraic equations (SLAE) by minimizing the mean square deviation of $U(\alpha)$ (4) from the received signal (2) [16–23]:

$$V = HB, \quad (5)$$

$$V_n = \int_{\Omega} U(\alpha) G_n(\alpha) d(\alpha), \quad H_{n,m} = \int_{\Omega} G_m(\alpha) G_n(\alpha) d(\alpha), \quad n, m = 1, \dots, M. \quad (6)$$

If the signal is given as a discrete sequence of values, the problem reduces to solving an overdetermined SLAE based on the least squares method.

The boundaries of the angular sector Ω , within which signal sources are located, are initially chosen based on an estimate, considering a significant decrease in the level of the received signal at the boundaries of Ω relative to its maximum value. Later, based on preliminary solutions, the boundaries of sector Ω are refined, and the solution is sought in a new, usually smaller, angular sector. As numerical experiments have shown, after several iterations, the size and boundaries of sector Ω become close to the true ones.

The choice of the system of functions $g_m(\alpha)$ for representing the solution (3) is based on using a priori information about signal sources or, in its absence, on a reasonable model of physically realizable source types.

Enhancing the achievable super-resolution level is based on increasing the number of functions in the representation (3). However, in the considered inverse problems, matrices H in SLAE (5) are ill-conditioned. Their condition numbers grow exponentially with increasing matrix dimension. A stable approximate solution for UAV-type signal sources can only be obtained for the first few functions from (3), which, at high SNR, allows exceeding the Rayleigh criterion by 2–4 times [10, 13, 14].

To further improve the quality of the approximate solution by increasing the number of used functions in (4)–(6), it is proposed to apply Tikhonov regularization method [16] to the stated problem (2).

Formally, solving SLAE (5) is equivalent to minimizing the function

$$\Phi(B) = \|HB - V\|^2, \quad (7)$$

where $\|\cdot\|$ denotes the vector or matrix norm. The Tikhonov regularization method allows finding the normal solution of system (5) using representation (7), i.e., the vector B minimizing the norm of vector $\|HB - V\|$.

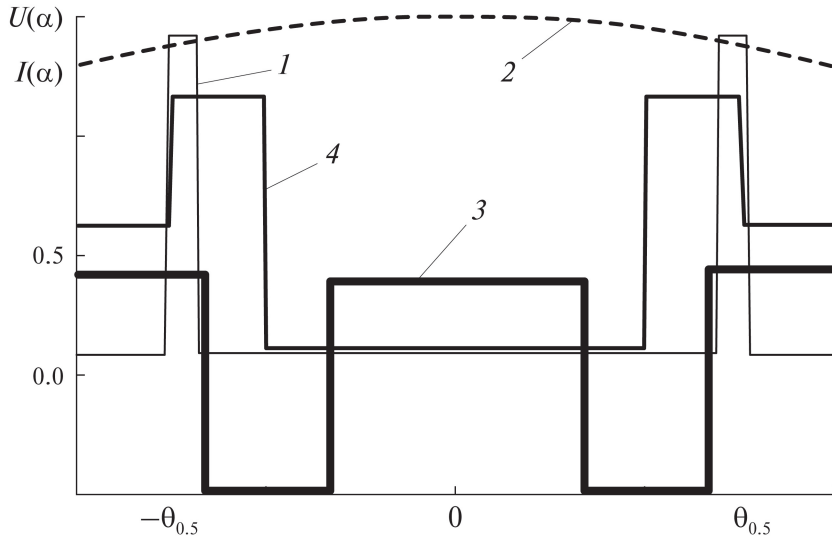


Fig. 1. Solution of the problem for two close objects.

The solution consists in finding the vector B for which the function

$$\Phi(B, \lambda) = \|HB - V\|^2 + \lambda \|B\|^2 \quad (8)$$

reaches the smallest value for a fixed positive λ . It is known that a solution to such a problem exists and is unique [16].

The problem of minimizing function $\Phi(B, \lambda)$ (8), as can be easily shown, is equivalent to solving the SLAE

$$(H^T H + \lambda E)B = H^T V, \quad (9)$$

where E is the identity matrix, H^T is the transposed matrix. For $\lambda = 0$, equation (9) transforms into the original SLAE.

The Tikhonov regularization method additionally allows accounting for a possible a priori approximate estimate of the solution, given in the form of expected coordinates of vector B as a vector C .

Then instead of (8), (9) we obtain

$$\begin{aligned} \Phi(B, \lambda) &= \|HB - V\|^2 + \lambda \|B - C\|^2, \\ (H^T H + \lambda E)B &= H^T V + \lambda C. \end{aligned} \quad (10)$$

Since in solving real problems related to measurement systems, the input data always contain random components, to choose the best solution, it is necessary to perform calculations for various values of the regularization parameter λ , close to the level of random components in the studied signal. As a model example, the problem of achieving angular super-resolution for two closely located identical small-size objects at high SNR was solved.

In Figs. 1 and subsequent figures, the zero direction is taken as the direction to the antenna plane; the vertical axis—the amplitude value of signal sources and the received signal, normalized to unity; the horizontal axis—the scanning angle α of the system in relative units of $\theta_{0.5}$ beamwidth; true signal sources, simulating UAVs, are shown as a thin black solid broken line (curve 1). The angular dependence of the received signal $U(\alpha)$, showing that during direct observation without signal processing the sources merge into a single object, is presented by a dashed curve (curve 2). The thick

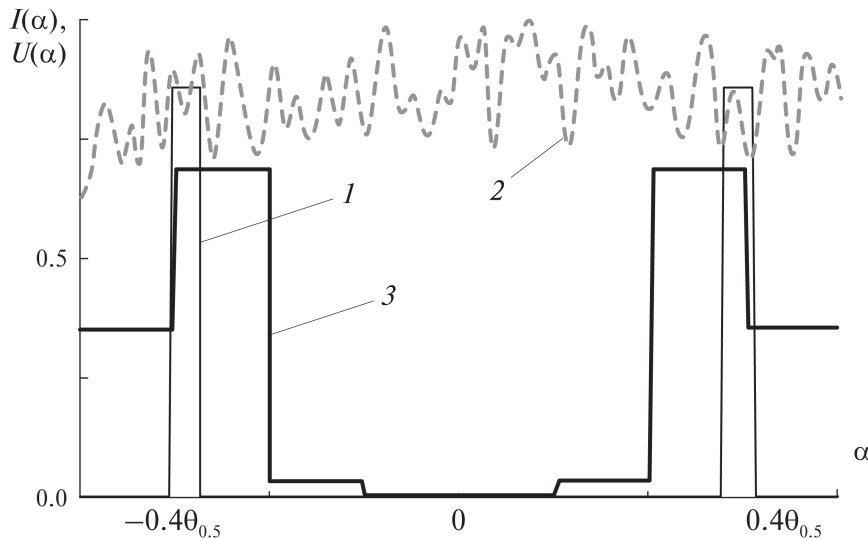


Fig. 2. Solution of the problem for two close objects, SNR = 12dB: 1—true sources, 2—received signal $U(\alpha)$, 3—solution with super-resolution.

stepped line 3 is the solution by the algebraic method (3)–(6) without problem regularization. The obtained inadequate solution is unstable and represents an oscillating function. The broken curve 4 is the stable solution obtained using Tikhonov regularization. Both true sources are observed separately. The Rayleigh criterion is exceeded by a factor of 5.

When comparing super-resolution achievement methods, one of the main quality criteria is the dependence of the degree of exceeding the Rayleigh criterion on SNR. This is because inverse problems are being solved, which are significantly more sensitive to the level of random components in the studied signals than direct problems. By this criterion, Tikhonov regularization allows sharply improving the quality of the obtained solutions.

On Fig. 2, the solution of the same problem is presented in the same notations as in Fig. 1, but at SNR = 12 dB. The obtained stable solution practically did not change, whereas for popular super-resolution achievement methods [1–7] the minimally required SNR level is 20 dB.

4. REGULARIZATION OF THE PROBLEM BY THE SEPARATION METHOD

Suppose that from a group target, using M step functions, it was possible to isolate K separate objects (or one object) and approximately determine their angular positions and amplitudes of reflected signals. Then the number of objects in the new group target will be $M - K$. For the isolated K objects, we assume that their locations $g_k(\alpha)$ and amplitudes b_k have been found:

$$I_k(\alpha) = b_k g_k(\alpha), \quad k = M - K + j, \quad j = 1, \dots, K. \quad (11)$$

The problem arises of separating the remaining objects in the new group. For this, a method based on extracting from the received reflected signals $U(\alpha)$ only those that belong to the new group target is proposed.

The signal received from the already isolated K sources

$$U_K(\alpha) = \sum_{k=P}^M \int_{\Gamma} F(\alpha - \alpha') I_k(\alpha') d\alpha' = \sum_{k=P}^M b_k \int_{\Gamma} F(\alpha - \alpha') g_k(\alpha') d\alpha' = \sum_{k=P}^M b_k G_k(\alpha), \quad (12)$$

where $P = M - K + 1$, Γ is the region of location of the isolated sources. For the new problem, signal $U_K(\alpha)$ becomes interference, and strong interference at that, which prevents isolating individual sources from the new group.

It is possible to largely neutralize the influence of this interference. For this, from the received real signal $U(\alpha)$, one should subtract an artificially synthesized signal imitating the signal from the previously separated K sources (12). Then the signal received from the remaining objects, representing the new group target of P objects, becomes equal to

$$U_S(\alpha) = U(\alpha) - U_K(\alpha). \quad (13)$$

The formed signal in the form (13) can be further used in solving the super-resolution achievement problem for the new group target similarly to (3)–(6). Introducing a new system of step functions $h_m(\alpha)$ for this, we finally obtain an SLAE of the form

$$W = QC, \quad (14)$$

where the elements of vector W and matrix Q are represented as:

$$\begin{aligned} W_k &= \int_{\Phi} U_S(\alpha) H_k(\alpha) d\alpha, & Q_{k,q} &= \int_{\Phi} H_k(\alpha) H_q(\alpha) d\alpha, \\ H_k(\alpha) &= \int_{\Phi} F(\alpha - \alpha') h_k(\alpha') d\alpha'. \end{aligned} \quad (15)$$

Here C is the vector with elements b_k from (11), Φ is the region of location of the new group target.

Estimation of the position and boundaries of region Φ is now performed based on analysis of the synthesized signal $U_S(\alpha)$ similarly to determining region Ω in (6). If the previously separated K objects are located near the boundary of region Ω , then the size of region Φ becomes smaller than Ω . If the separated objects are not located at the edge of the region, then the new region Φ also turns out to be smaller than Ω , but doubly connected or even multiply connected. Constructing a solution in a multiply connected region is performed according to the same scheme as in the one-dimensional case, by introducing a finite system of functions orthogonal in region Φ .

In the new reduced region Φ , the same number of functions $g_m(\alpha)$ as in region Ω in (3) provides greater resolution without a substantial increase in the condition numbers of matrix H in (5). In many cases, this allows angular resolution of objects of the new group target. The described approach to the problem of analyzing a UAV swarm or other objects constituting a group target can be called the *separation method*.

5. SEPARATION METHOD

It should be noted that the coefficients b_m from (5), (6), and consequently $U_S(\alpha)$, are found with some error. For direct problems, the error may be insignificant and can be neglected. However, the considered problem is inverse, the stability of its solutions is significantly worse. To obtain adequate results, it is necessary to refine the values of b_m before their further use in (7)–(15).

Refinement of the values is proposed to be carried out according to the following scheme. Problem (3)–(6) is solved, but instead of signal $U(\alpha)$, signal $U_S(\alpha)$ is used, i.e., vector V is replaced by vector W from (10). In the idealized case, i.e., if coefficients b_m and $U_S(\alpha)$ were previously found accurately, all coefficients b_k in (7) turn out to be zero.

In the real case, we obtain values b_m and b_k satisfying the relation

$$U_S(\alpha) = U(\alpha) - \sum_{k=M-K+1}^K b_k^0 G_k(\alpha) = \sum_{m=1}^{M-K} b_m^1 G_m(\alpha) + \sum_{k=M-K+1}^M b_k^1 G_k(\alpha), \quad (16)$$

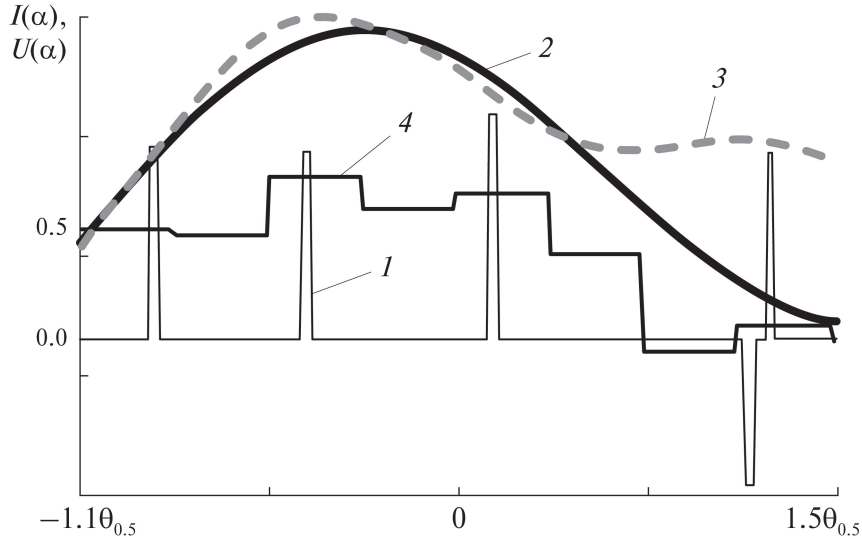


Fig. 3. Separation of one object from a group target. 1—True sources, 2—synthesized signal $U_S(\alpha)$, 3—received signal, 4—solution with super-resolution.

where b_k^0 are the values of b_k , found with some error when solving problem (8)–(15) with the original signal $U(\alpha)$, b_m^1 are refined values of coefficients b_m when solving the problem with the original signal $U_S(\alpha)$, b_k^1 are residual values of coefficients b_k not equal to zero, arising due to errors in determining b_k^0 .

To reduce these errors, an iterative process [17] is then built. Instead of coefficients b_k^0 in (8) at the first step, we use $\tilde{b}_k^1 = b_k^0 + b_k^1$, and instead of $U_S(\alpha)$ in the form (9) $U_S^1(\alpha)$ i.e.

$$U_S(\alpha) = U(\alpha) - U_K(\alpha), \quad U_K^1(\alpha) = \sum_{k=M-K+1}^M \tilde{b}_k^1 G_k(\alpha). \quad (17)$$

Further, similarly to (14), (15), we obtain the second approximation b_k^2 . At the next step, we use $\tilde{b}_k^1 = b_k^0 + b_k^1 + b_k^2$, etc. At the n th step, we arrive at the relation

$$U_S^n(\alpha) = U(\alpha) - U_K(\alpha), \quad U_K^1(\alpha) = \sum_{k=M-K+1}^M \tilde{b}_k^1 G_k(\alpha). \quad (18)$$

Numerical experiments showed that in several iterations b_k^n decrease significantly compared to the initial values and become comparable to errors in the input data.

As an example of applying the separation method, consider a group target of four point objects located in the angular sector $[-1.1\theta_{0.5}; 1.5\theta_{0.5}]$, with small differences in signal amplitude values.

In Fig. 3, the original angular dependence of the received signal $U(\alpha)$ is shown as a dashed curve (curve 3). The objects are not angularly resolved by direct observation. Solution by the algebraic method (3)–(6) using eight step functions allowed isolating one object from the group target.

Using a larger number of functions leads to unstable inadequate solutions that cease to reflect reality. Such solutions can be easily recognized, as coefficients b_m begin to take values orders of magnitude larger than real ones.

The degree of solution stability can be assessed using condition numbers of matrices H from (5). Note that condition numbers of such matrices increase sharply (exponentially) with an increase in the number of used functions. Consequently, the number of functions $g_m(\alpha)$ in representing solution (3) is always limited.

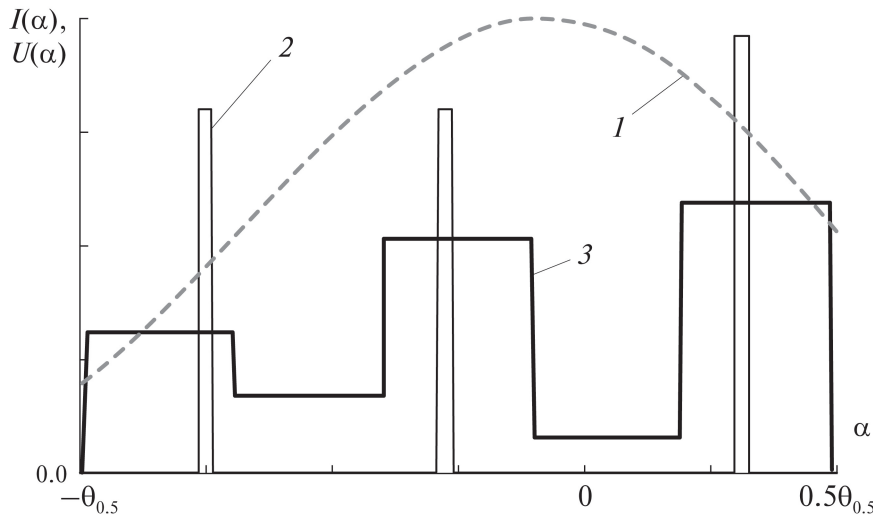


Fig. 4. Solution of the problem based on the object separation method.

Figure 3 shows: as a thin broken line (curve 1)—positions of true point signal sources and the introduced virtual source $I_N(\alpha)$ (12) with negative polarity; as a thick solid curve (curve 2)—the synthesized signal $U_S(\alpha)$, which was used to refine the signal amplitude reflected by the fourth object, i.e., refining b_4 ; dotted curve (curve 3)—the reflected signal; as a thick stepped curve (curve 4)—the solution of the inverse problem (2) based on the synthesized signal $U_S(\alpha)$ in the original region Ω .

The solution confirmed the correctness of isolating one object from the group target. However, resolving the remaining objects in angle using the eight introduced step functions $g_m(\alpha)$ in Ω was not possible.

In this case, one should proceed to the second stage of solving the problem by the separation method in the found new region Φ (15).

The second stage consists in using $U_S^n(\alpha)$ instead of $U_S(\alpha)$ in (13)–(15) for the newly formed group target.

On Fig. 4, the solution results are presented. As a thick dashed curve (curve 1), the synthesized signal $U_S^n(\alpha)$ (18) is shown. Thin broken line (curve 2)—true point signal sources, thick solid broken line (curve 3)—the found solution using five step functions $g_m(\alpha)$ in region Φ , the size of which turned out to be 1.75 times smaller than the original region Ω .

Sufficient solution stability and the achieved super-resolution level in the considered example allowed separately registering and determining the coordinates of all objects in the new group target.

The second stage of solution does not always allow resolving objects of the group target. For each specific target and specific measurement system, there exists an angular distance between objects below which their resolution is impossible.

6. NONLINEAR REGRESSION

In cases where resolving objects of a group target using the proposed methodology fails, a more complex approach is proposed in the comprehensive method.

Note that the above separation method is based on determining object amplitudes b_j with high accuracy. However, the accuracy of the angular position of each object does not change, as it is

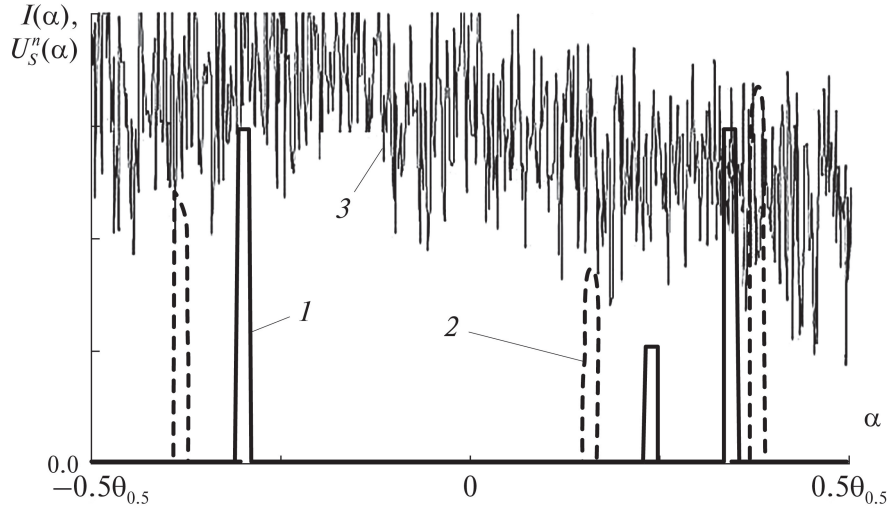


Fig. 5. Solution of the problem for a group target using nonlinear regression.

limited by the angular size of the used step function. More accurate determination of coordinates α_j simultaneously with searching for b_j will improve the quality of obtained solutions.

Assume, as in the given examples, that angular coordinates of objects are negligibly small and can be described using delta-functions $\delta(\alpha - \alpha_j)$, where α_j is the coordinate of the j th object, $j = 1, \dots, N$, $N = M - K$. Then instead of (3)–(4) we obtain further (19)–(20)

$$I(\alpha) = \sum_{m=1}^N \delta(\alpha - \alpha_m), \quad (19)$$

$$U_S^n(\alpha) = \sum_{m=1}^N F(\alpha - \alpha_m). \quad (20)$$

Search for new refined solutions α_j and b_j is proposed to be carried out based on applying nonlinear regression [25–29]. We introduce a regression function similar to (16), i.e.

$$L(\alpha) = \sum_{m=1}^N d_m F(\alpha - \gamma_m), \quad (21)$$

where γ_m and d_m are the desired parameters. We also use an additional condition in the form of equality of received signal powers

$$\int_{\Phi} \left(U_S^n(\alpha) \right)^2 d\alpha = \int_{\Phi} \left(\sum_{m=1}^N d_m F(\alpha - \gamma_m) \right)^2 d\alpha. \quad (22)$$

Solution based on minimizing the mean square deviation of (21) from $U_S^n(\alpha)$ reduces to solving a system of nonlinear equations. Then, using standard nonlinear regression algorithms, we determine unknown parameters γ_m and d_m minimizing the deviation.

Numerical search for solutions for several objects does not cause significant difficulties, since a good initial approximation is used in the form of previously found b_m and coordinates α_m specified within each previously used step function.

On Fig. 5, an example of solving the problem for three closely located objects with different amplitudes of reflected signals is given. The real location of point sources and their amplitude

values are shown by solid broken lines (curve 1). The useful signal $U_S^n(\alpha)$ received during scanning together with the noise component within angles $[-\theta_{0.5}/2, \theta_{0.5}/2]$ is shown as a rapidly oscillating curve (curve 3). Using the previously described methods did not allow resolving the targets. Using nonlinear regression allowed obtaining an adequate solution, shown by a dashed broken line (curve 2).

All objects are resolved, their location is determined with good accuracy, amounting to 0.07 beamwidth. Amplitude values were found with less accuracy, but they are of secondary importance. The resolution exceeded the Rayleigh criterion by more than four times.

Solving the system of nonlinear equations based on (19)–(22) is noticeably more stable than solving SLAE (14). Numerical experiments showed that adequate solutions are obtained at SNR down to 18 dB, i.e., at higher levels of random components than when using known super-resolution methods.

In some cases, when UAVs are located with high density, resolving objects by the methods described above fails. However, through a more complex approach and some complication of the technical system, achieving super-resolution is possible in these cases as well. For this, it is proposed to use a so-called *harmonic radar*.

7. NONLINEAR SECONDARY RADAR

Secondary, or harmonic radar (HR), upon reception uses a signal frequency two or three times higher than the probing (or interrogation) signal frequency. The received signal is formed due to reflection from nonlinear elements of the studied objects. As a result, the signal represents a superposition of harmonics, multiples of the emitted frequency [24–29].

Ordinary radar objects exhibit nonlinear properties to a very small degree. Currently, HR with specially built-in nonlinear elements are most often used in rescue operations under complex conditions on land and sea for searching and measuring coordinates of objects.

In the considered problems, in the studied angular region at the emitted frequency f_0 , there are many signals reflected from a large number of objects, including dangerous mobile objects. Moreover, signals can represent interference at the used frequency f_0 , including intentionally created ones. Ultimately, determining coordinates of individual objects by analyzing the total response signal at frequency f_0 turns out to be practically impossible.

At the same time, nonlinear HR detects only targets possessing nonlinear properties, using frequencies $2f_0$ and $3f_0$, and any signals and interference at frequency f_0 do not affect its operation.

The main disadvantage of HR is the weak reflected signal at the used, multiples of f_0 , frequencies compared to reflection at the original frequency f_0 . This circumstance significantly limits the range D of nonlinear radars. Various methods are proposed to increase it [24–29]. Ultimately, at frequencies $2f_0$ and $3f_0$, a range up to $D \sim 1\text{--}5$ km can be achieved.

Ensuring determination of coordinates of individual objects is possible when reducing the number of objects in the studied region. For this, it is proposed to install lightweight small-size nonlinear elements on certain types of UAVs. Simple antennas, including printed ones, in the form of dipoles with a diode, can be used as such. Then, against the background of signals reflected by them at frequencies $2f_0$ and $3f_0$, other UAVs will become practically unnoticeable.

In this case, it becomes possible to measure coordinates of selected types of UAVs at frequencies $2f_0$ and $3f_0$, including using super-resolution methods if necessary. At the main frequency f_0 , the above-described method of separating objects in the form of selected types of UAVs with now known coordinates becomes applicable. Consequently, the number of UAVs in the surveillance zone decreases, and the problem of determining coordinates of the remaining UAVs of other types is simplified. Its solution is now carried out according to the above scheme (3)–(6) and (7)–(10).

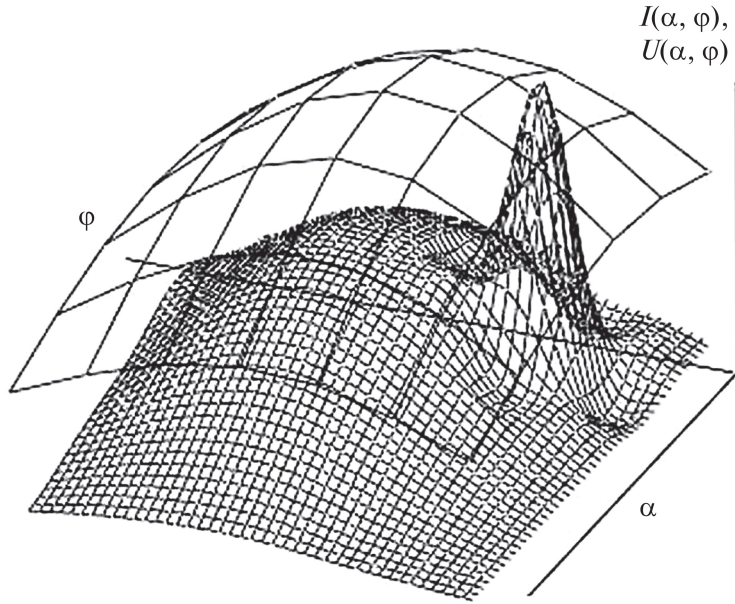


Fig. 6. Improving the accuracy of angular measurements of airborne radars.

Low accuracy of angular measurements for aerial vehicles of relatively small size in autonomous mode at frequencies $2f_0$ and $3f_0$ can significantly reduce the effectiveness of using the presented separation method. This drawback can be largely compensated by using algebraic signal processing methods of airborne radars (3)–(6) to achieve super-resolution at frequencies $2f_0$ and $3f_0$. An example of such compensation is given in Fig. 6.

As a sparse grid, the two-dimensional received signal $U(\alpha, \varphi)$ at frequency $2f_0$ is shown. The true distribution of the emitted signal amplitude was a point source and a small background emission at the second harmonic. When solving direct problems, the background emission can be neglected without any noticeable error. However, when solving inverse unstable problems in the form of IE (2), it can noticeably distort solutions.

The received signal $U(\alpha, \varphi)$ very roughly estimates the angular coordinates of the source. In the considered problem, this is the region covered by the sparse grid. The approximate solution found by the algebraic method (4)–(6), i.e., distribution $I(\alpha, \varphi)$ considering the interfering background emission, is shown as a dense grid. The obtained solution of the IE shows that the point source is located within the peak of $I(\alpha, \varphi)$.

The accuracy of determining the coordinates of signal sources and its localization improved by more than five times. Noise in the form of background emission slightly distorted the true solution and did not allow obtaining even more accurate source coordinates.

For HR, further improvement of angular measurement accuracy and angular resolution is possible. For this, one should simultaneously analyze received signals at the second $U_2(\alpha, \varphi)$ and third $U_3(\alpha, \varphi)$ harmonics. The simplest method of analysis is summing the amplitudes of these signals during scanning:

$$\begin{aligned} U(\alpha, \varphi) &= U_2(\alpha, \varphi) + kU_3(\alpha, \varphi) \\ &= \int_{\Omega} [f_2(\alpha - \alpha', \varphi - \varphi')I_2(\alpha', \varphi') + kf_3(\alpha - \alpha', \varphi - \varphi')I_3(\alpha', \varphi')] d\alpha' d\varphi', \end{aligned} \quad (23)$$

where $I_2(\alpha, \varphi)$ and $I_3(\alpha, \varphi)$ describe the same angular position of the source but with different amplitude values. For signals at the third harmonic, a gain coefficient k is introduced. Since the

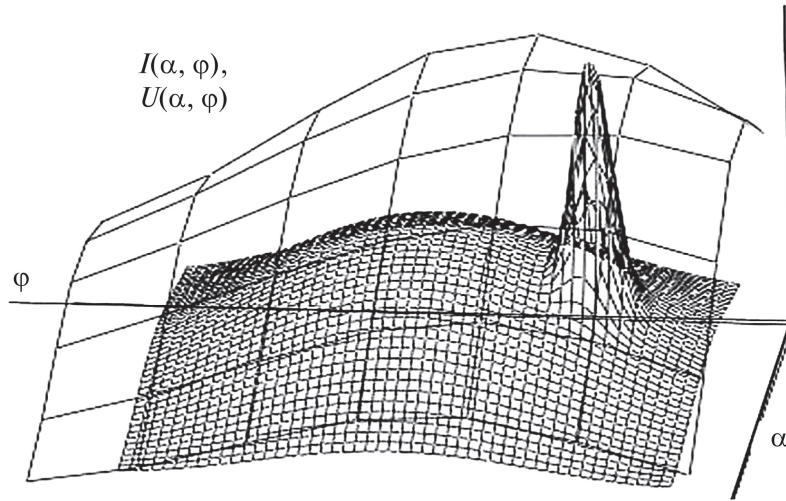


Fig. 7. Solution of IE for the sum of two harmonics.

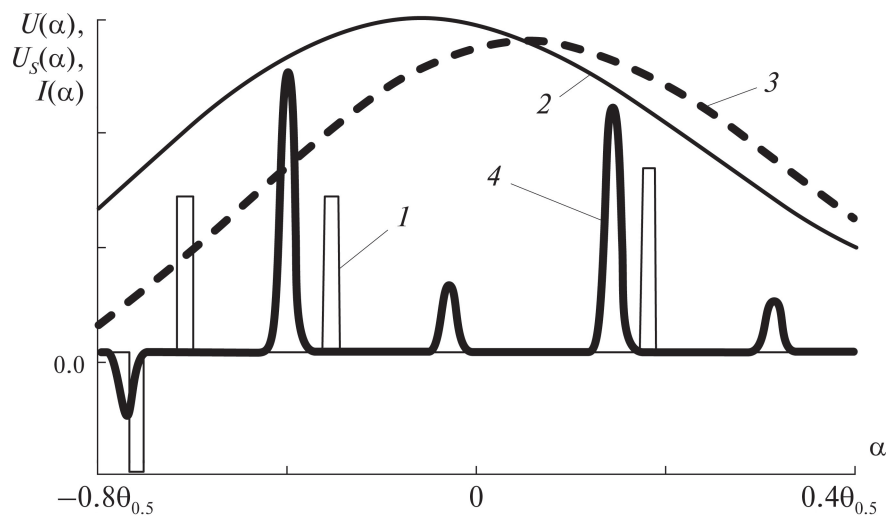


Fig. 8. Solution when separating one object of known type. The solution of the problem of determining angular coordinates of a complex object using HR is presented. The object represented a group target consisting of three closely located point targets—thin broken line (curve 1). The original signal $U(\alpha)$ (2) is shown as a thin smooth curve (curve 2).

amplitude of signals at the third harmonic is significantly lower than at the second, coefficient k is chosen from the condition of approximate equality of maximum values of $U_2(\alpha, \varphi)$ and $U_3(\alpha, \varphi)$. The condition of equality of maxima ensures approximately equal contribution of harmonics to the desired solution. An additional advantage of summing harmonics is that noises present in signals $U_2(\alpha, \varphi)$ and $U_3(\alpha, \varphi)$ are non-coherent, and their addition ensures an increase in SNR in (23) compared to SNR at each of frequencies $2f_0$ and $3f_0$. In Fig. 7, results of solving IE (23) for the same problem as in Fig. 6 are shown, in the same notations. As expected, the localization accuracy of the true source noticeably increased—by a factor of two. This ensured an improvement in the accuracy of solving the problem of separating an object of known type from a group target. Resolving targets is not possible either by direct observation or using known super-resolution methods.

One of the objects, namely the one located close to the left boundary of zone Ω , at frequencies $2f_0$ and $3f_0$, is identified by HR as an object of known type. At these frequencies, its angular

coordinate α_1 is measured. According to the separation method (12)–(14) at frequency f_0 , a compensating signal with negative polarity is synthesized:

$$U_S(\alpha) = U(\alpha) - AF(\alpha_1). \quad (24)$$

The reflection coefficient A at frequency f_0 is not known in advance and is initially set based on a reasonable estimate. Then it is subject to refinement during the iterative process of solving the problem similar to (16)–(18).

The final signal $U_S(\alpha)$ (14) is shown in Fig. 8 as a thick dashed curve (curve 3).

For representing the solution, Gaussian functions were used as functions $g_m(\alpha)$ in (3). The found solution without the previously identified UAV with angular coordinate α_1 is shown as a thick curve (curve 4). In the final solution, the source was represented as a superposition of five Gaussian functions $g_m(\alpha)$:

$$I(\alpha) = \sum_{m=1}^5 b_m g_m(\alpha - \Delta\alpha m) \quad (25)$$

with distance $\Delta = 0.23\theta_{0.5}$ between maxima of adjacent $g_m(\alpha)$.

True, near-point signal sources together with the virtual compensating source $A\delta(\alpha - \alpha_1)$ are shown as a thin broken line (curve 1).

The appearance in the solution of many small objects, the radiation intensity $I^2(\alpha)$ of which is an order of magnitude lower than that of the others, is usually caused by the influence of noise and interference. Such targets are considered false.

Consequently, the obtained solution allowed resolving all objects of the group target and determining their angular coordinates with good accuracy.

8. CONCLUSION

1. A new comprehensive method for digital processing of radar signals reflected from multiple objects is theoretically justified and tested in numerical experiments. The method allows measurement systems to achieve angular resolution significantly exceeding the Rayleigh criterion.

2. The proposed separation method, as shown by analytical and numerical results, is applicable for detecting and determining coordinates of individual objects within group targets, including those consisting of UAV “swarms.” Creating an artificially synthesized signal during processing of the obtained information allows substantially increasing the achievable super-resolution level compared to known methods.

3. New signal processing algorithms based on nonlinear regression methods allow improving the accuracy of determining angular coordinates and enhancing localization of studied objects by 2–5 times.

4. Using mathematical models, it is shown that nonlinear regression methods allow solving super-resolution achievement problems at higher levels of noise and interference than known methods.

5. The use of harmonic radar for achieving angular resolution allowing the isolation of dangerous UAVs within group targets is justified.

6. Algorithms based on the proposed comprehensive method are relatively simple and can be applied in real time.

FUNDING

The work was partially supported by the Russian Science Foundation (project no. 23-29-00448).

REFERENCES

1. Morse, P. and Feshbach, H., *Methods of Theoretical Physics*, McGraw-Hill, 1953.
2. Uttam, S. and Goodman, N.A., Superresolution of coherent sources in real-beam Data, *IEEE Trans. Aerosp. Electron. Syst.*, 2010, vol. 46, no. 3, pp. 1557–1566.
3. Park, S.C., Park, M.K., and Kang, M.G., Super-resolution image reconstruction: a technical overview, *IEEE Signal Process. Mag.*, 2003, vol. 20, no. 3, pp. 21–36.
4. Kasturiwala, S.B. and Ladha, S.A., Superresolution: A novel application to image restoration, *Int. J. Comput. Sci. Eng.*, 2010, no. 5, pp. 1659–1664.
5. Waweru, N.P., Konditi, D.B.O., and Langat, P.K., Performance analysis of MUSIC Root-MUSIC and ESPRIT, *Int. J. Electr. Comput. Energ. Electron. Commun. Eng.*, 2014, vol. 8, no. 1, pp. 209–216.
6. Lavate, T.B., Kokate, V.K., and Sapkal, A.M., Performance analysis of MUSIC and ESPRIT, *Proc. 2nd Int. Conf. Comput. Netw. Technol. (ICCNT)*, 2010, pp. 308–311.
7. Almeida, M.S. and Figueiredo, M.A., Deconvolving images with unknown boundaries using the alternating direction method of multipliers, *IEEE Trans. Image Process.*, 2013, vol. 22, no. 8, pp. 3074–3086.
8. Evdokimov, N.A., Lukyanenko, D.V., and Yagola, A.G., Application of multiprocessor systems to solving the two-dimensional convolution-type Fredholm integral equations of the first kind for vector-functions, *Numer. Methods Program.*, 2009, vol. 10, p. 263.
9. Lagovsky, B.A. and Rubinovich, E.Y., Algebraic methods for achieving superresolution by digital antenna arrays, *Mathematics*, 2023, vol. 11, no. 4, pp. 1–9. <https://doi.org/10.3390/math11041056>
10. Lagovsky, B., Samokhin, A., and Shestopalov, Y., Angular Superresolution Based on A Priori Information, *Radio Sci.*, 2021, vol. 5, no. 3, pp. 1–11. <https://doi.org/10.1029/2020RS007100>
11. Lagovsky, B.A. and Rubinovich, E.Y., A modified algebraic method of mathematical signal processing in radar problems, *Results Control Optim.*, 2024, vol. 14, no. 3, p. 100405. <https://doi.org/10.1016/j.rico.2024.100405>
12. Alexandrov, A.E., Borisov, S.P., Bunina, L.V., Bikovsky, S.S., Stepanova, I.V., and Titov, A.P., Statistical model for assessing the reliability of non-destructive testing systems by solving inverse problems, *Russ. Technol. J.*, 2023, vol. 11, no. 3, pp. 56–69.
13. Lagovsky, B. and Rubinovich, E., Algorithms for Digital Processing of Measurement Data Providing Angular Superresolution, *Mekhatronika, Avtomatizatsiya, Upravlenie*, 2021, vol. 22, no. 7, pp. 349–356.
14. Lagovsky, B. and Rubinovich, E., Achieving Angular Superresolution of Control and Measurement Systems in Signal Processing, *Adv. Syst. Sci. Appl.*, 2021, vol. 21, no. 2, pp. 104–116.
15. Lagovsky, B.A. and Rubinovich, E.Y., A modified algebraic method of mathematical signal processing in radar problems, *Results Control Optim.*, 2024, vol. 14, no. 3, p. 100405. <https://doi.org/10.1016/j.rico.2024.100405>
16. Tikhonov, A.N. and Arsenin, V.Y., *Methods for Solving Ill-Posed Problems*, Nauka, 1979.
17. Lagovsky, B.A. and Rubinovich, E.Y., Enhancing angular resolution and range of measurement systems using ultra-wideband signals, *Avtom. Telemekh.*, 2023, no. 10, pp. 72–90. <https://doi.org/10.31857/S0005231023100070>
18. Kelley, C.T., *Iterative Methods for Optimization*, SIAM, 1999.
19. Marquardt, D.W., An Algorithm for Least-Squares Estimation of Nonlinear Parameters, *J. Soc. Ind. Appl. Math.*, 1963, vol. 11, no. 2, pp. 431–441. <https://doi.org/10.1137/0111030>
20. Lourakis, M.I.A. and Argyros, A.A., Is Levenberg-Marquardt the Most Efficient Optimization Algorithm for Implementing Bundle Adjustment, *Proc. 10th IEEE Int. Conf. Comput. Vis. (ICCV)*, 2005, pp. 1526–1531. <https://doi.org/10.1109/ICCV.2005.128>
21. Nocedal, J. and Wright, S.J., *Numerical Optimization*, Springer, 2006. <https://doi.org/10.1007/978-0-387-40065-5>

22. Seber, G.A.F. and Wild, C.J., *Nonlinear Regression*, Wiley, 1989.
23. Oosterbaan, R.J., Frequency and Regression Analysis, in *Drainage Principles and Applications*, H.P. Ritzema, Ed., ILRI, 1994, vol. 16, pp. 175–224.
24. Lavrenko, A., Cavers, J.K., and Woodward, G.K., Harmonic Radar With Adaptively Phase-Coherent Auxiliary Transmitters, *IEEE Trans. Signal Process.*, 2022, vol. 70, pp. 1788–1802.
<https://doi.org/10.1109/TSP.2022.3164183>
25. Harzheim, T., Muhmel, M., and Heuermann, H., A SFCW harmonic radar system for maritime search and rescue using passive and active tags, *Int. J. Microw. Wirel. Technol.*, 2021, vol. 13, no. 7, pp. 691–707.
<https://doi.org/10.1017/S1759078721000520>
26. Mazzaro, G.J. and Martone, A.F., Multitone harmonic radar, *Proc. SPIE*, 2013, vol. 8714, p. 87140E.
<https://doi.org/10.1117/12.2014241>
27. Kumar, D., Mondal, S., Karuppuswami, S., Deng, Y., and Chahal, P., Harmonic RFID communication using conventional UHF system, *IEEE J. Radio Freq. Identif.*, 2019, vol. 3, no. 4, pp. 227–235.
28. Mondal, S., Kumar, D., and Chahal, P., Recent advances and applications of passive harmonic RFID systems, *Micromachines*, 2021, vol. 12, no. 4, pp. 1–22.
29. Viikari, V., Sepp, H., and Kim, D.-W., Intermodulation read-out principle for passive wireless sensors, *IEEE Trans. Microw. Theory Tech.*, 2011, vol. 59, no. 4, pp. 1025–1031.

This paper was recommended for publication by B.M. Miller, a member of the Editorial Board